Acta Crystallographica Section B
Structural Science
ISSN 0108-7681

Use of the Inorganic Crystal Structure Database as a problem solving tool

James A. Kaduk

BP Chemicals, PO Box 3011, MC F-9, Naperville, IL 60566, USA

Correspondence e-mail: kadukja@bp.com

Received 1 February 2002
Accepted 21 February 2002

The information in the Inorganic Crystal Structure Database (ICSD) can be used to determine the structures of new compounds by analogy; this database is thus a useful tool for practical problem solving. A model for the structure of $(NH_4)Fe(CO_3)(OH)_2$ [*Cmcm*, a = 6.6154 (6), b = 12.0639 (10), c = 6.0263 (5) Å, Z = 4] was found by searching the ICSD for compounds with *C*-centered orthorhombic cells and containing C, H, N and O. $[Al(H_2O)_6]_2[Al(H_2O)_5(SO_4)]_2(H_3O)_2(SO_4)_5$ [$P\bar{1}$, a = 12.5881 (5), b = 13.0726 (5), c = 7.3354 (2) Å, α = 108.162 (2), β = 70.536 (2), γ = 112.658 (2)°, Z = 1] is isostructural to a Cr compound of the same stoichiometry, which was located by searching on the formula type ANX = A4B7X52. Suitable models for $MgCl_2(H_2O)_4$ [$P2_1/c$, a = 5.9001 (9), b = 7.2709 (7), c = 8.4199 (7) Å, β = 111.007 (15)°, Z = 2], $MgCl_2(H_2O)_2$ [$C2/m$, a = 7.3886 (29), b = 8.5498 (24), c = 3.6488 (17) Å, β = 98.96 (3)°, Z = 2], and $MgCl_2(H_2O)$ [*Pnma*, a = 8.899 (7), b = 3.6339 (20), c = 11.398 (8) Å, Z = 4] were located by combining searches on chemistry and formula type. Quantum-chemical calculations were performed on all five structures to locate the H-atom positions and to obtain quantitative understanding of the hydrogen bonding important in all the structures.

1. Introduction

We normally think of the structural databases, the Inorganic Crystal Structure Database (ICSD; Bergerhoff *et al.*, 1983; Belsky *et al.*, 2002), the Cambridge Structural Database (CSD; Allen, 2002; Bruno *et al.*, 2002), CRYSTMET (White *et al.*, 2002) and the Protein Data Bank (PDB; Berman *et al.*, 2002), as archives of atomic coordinates. While the coordinates are useful in research and as input to Rietveld refinements (for quantitative phase analysis and other purposes), both they and the other information in the databases are useful for solving practical problems. In this paper, examples are described of using the ICSD to solve several problems which arose in support of operations.

2. $(NH_4)Fe(CO_3)(OH)_2$

2.1. Background

After the liquid-ammonia supply to one of BP Chemicals' plants was changed, deposits began to form in a liquid-ammonia heat exchanger. Such deposits reduce the efficiency of the exchanger, so identifying their nature (and thus their cause) had significant impact on process economics. These

deposits consisted of mixtures of phases, including the PDF (Powder Diffraction File, 2001; Faber & Fawcett, 2002) entry 22-52, '$(NH_4)_2Fe_2(OH)_4(CO_3)_2(H_2O)$' (Dvořák & Feitknecht, 1969). This compound (CAS Registry Number 12540-49-7) has been reported in only one other reference (Erdös & Altorfer, 1976) as a corrosion product of carbon steel in aqueous solutions of ammonia and carbonic acid. Because we perform almost all of our quantitative analysis using the Rietveld method, it was necessary to determine the crystal structure of this compound.

2.2. Preparation of the compound

This compound was prepared nearly phase-pure by the method of Dvořák & Feitknecht (1969). In a 250 ml polyethylene bottle, 20.097 g of NH_4HCO_3 (Fisher) were dissolved in 100 ml of distilled water. The solution cooled spontaneously and was brought to room temperature by gentle heating on a hot plate. Into this solution was added a solution of 0.3143 g of $Fe(NO_3)_3(H_2O)_9$ (Fisher) in 2.187 g of water; an orange effervescent solution resulted. This solution was magnetically stirred for 30 min, then the bottle was closed loosely and the solution stirred at room temperature for 2 d. The resulting light-yellow solid was filtered on Whatman #42 filter paper, washed with ethanol and air-dried. The product decomposes slowly on exposure to the air. The powder pattern (deposited as supplementary material along with the PDF entry used to identify the compound[1]), measured on a Scintag PAD V diffractometer equipped with an Ortec intrinsic Ge detector using Cu $K\alpha$ radiation from 3–100° 2θ in 0.02° steps for 12 s step^{-1}, agreed well with that reported by Dvořák & Feitknecht (1969).

2.3. Structure determination

The pattern could be indexed (Visser, 1969) on a *C*-centered orthorhombic unit cell having a = 6.6154 (6), b = 12.0639 (10) and c = 6.0263 (5) Å. A default search of the NIST Crystal Data Identification File (National Institute of Standards and Technology, 1997) yielded no hits. Both from the process chemistry and the PDF entry, we could reasonably assume that the compound contained C, H, N and O. A search of the ICSD for compounds containing these elements and having *C*-centered orthorhombic unit cells yielded 25 hits. Many of these could be discarded, as they were cyanide complexes. Among the hits was 'NH_4-dawsonite', $(NH_4)Al(CO_3)(OH)_2$ (Iga & Kato, 1978), which had also been reported as a corrosion product on aluminium by Erdös & Altorfer (1976). This compound crystallizes in space group *Cmcm*, with a = 6.618 (3), b = 11.944 and c = 5.724 (2) Å, thus representing a plausible structural model for the Fe analog. The bulk chemical analysis reported by Dvořák & Feitknecht (1969) accounts for only 86.5% of their product, suggesting that their formulation was incorrect.

[1] Supplementary data are available from the IUCr's electronic archives (Reference: AN0607). Services for accessing these data are described at the back of the journal.

2.4. Structure refinement

The model of Iga & Kato (1978) was used as the starting point for a Rietveld refinement using *GSAS* (Larson & Von Dreele, 1998). To minimize the effects of beam spill-over and surface roughness, only the 19–100° portion of the pattern was included in the refinement; the 22–24° region (which included an impurity peak) was excluded. All atoms were refined isotropically; the atoms of the carbonate were constrained to have the same U_{iso}. Soft constraints of 1.95 (1) Å were applied to the Fe—O bond distances, 1.28 (1) Å to the C—O bond distances, and 2.28 (2) Å to the carbonate O···O non-bonded distances. Hydrogen atoms were included in reasonable positions, which were not refined. A scale factor and the lattice parameters were refined. The slight preferred orientation (texture index = 1.029) was described using fourth-order symmetrized spherical harmonics. The peak profiles were described using the pseudo-Voigt profile function number 2. Only the Cauchy size broadening term X, the L_{xy} anisotropic strain broadening terms, and a specimen displacement coefficient were refined. The background was described by a three-term cosine Fourier series.

The final refinement of 32 variables using 3959 observations yielded the residuals R_{wp} = 0.0929, R_p = 0.0726, $R(F)$ = 0.0606, $R(F^2)$ = 0.0948, and χ^2 = 1.958. The largest peak and hole in the difference Fourier map were 0.74 and −0.82 electrons, respectively. The slope and intercept of the normal probability plot were 1.326 and 0.0726, respectively. The soft constraints contributed 5% to the final reduced χ^2. The agreement of the observed and calculated patterns (Fig. 1) is excellent.

Because it is difficult to locate and refine hydrogen-atom positions using laboratory X-ray powder data, and because hydrogen bonding is important in this structure, quantum-chemical optimizations of the structure were carried out using the Cambridge Serial Total Energy Package (*CASTEP*;

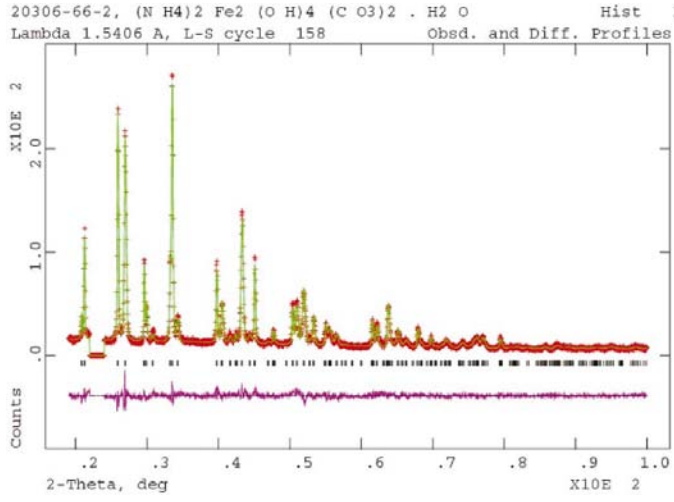

Figure 1
Observed, calculated and difference patterns of $(NH_4)Fe(CO_3)(OH)_2$. The small crosses represent the observed data points, and the smooth line through them the calculated pattern. The difference pattern is plotted at the same scale as the other patterns.

Table 1
Bond distances (Å) in $(NH_4)Fe(CO_3)(OH)_2$.

Fe1—O5 × 2	1.974 (2)	Fe1—O6 × 4	1.974 (2)
C3—O4	1.289 (4)	C3—O5 × 2	1.286 (2)

Table 2
Bond angles (°) in $(NH_4)Fe(CO_3)(OH)_2$.

O5—Fe1—O5	180	O6—Fe1—O6 × 2	180
O5—Fe1—O6 × 4	87.08 (13)	O5—Fe1—O6 × 4	92.92 (13)
O6—Fe1—O6 × 2	79.38 (13)	O6—Fe1—O6 × 2	100.62 (13)
O4—C3—O5 × 2	119.25 (27)	O5—C3—O5	121.5 (5)

Millman *et al.*, 2000). The lattice parameters were fixed, but the positions of all atoms were allowed to refine. The geometry optimization was carried out at the CGA-PW91 level of theory, with a 0.09 $Å^{-1}$ *k*-point spacing (two-point sampling of the Brillouin zone of the primitive unit cell). The compound was treated as a metal and the number of default orbitals was increased by 10% to include some empty orbitals in the calculation.

The refined and optimized atom coordinates and isotropic displacement coefficients are available in CIF format. Bond distances and angles are listed in Tables 1 and 2. The hydrogen bonds are described in Table 3. The calculated powder pattern of $(NH_4)Fe(CO_3)(OH)_2$ has been submitted to the International Centre for Diffraction Data for inclusion in future releases of the Powder Diffraction File.

2.5. Description of the structure

The crystal structure (Fig. 2) consists of chains (parallel to *c*) of edge-sharing octahedral Fe atoms (additional figures are available as supplementary material). The equatorial plane of the coordination sphere is composed of four bridging hydroxyl groups and the axial positions are occupied by bridging carbonate anions. All of the Fe—O bond lengths are 1.97 Å and the average deviation from the ideal octahedral angles is 6.5°. The largest deviations involve the hydroxyl groups, which alternate 'up' and 'down' along the chain. The bridging carbonates also alternate 'up' and 'down' along the chain, resulting in tilting of the FeO_6 octahedra. The angle between adjacent equatorial planes is 14.9°.

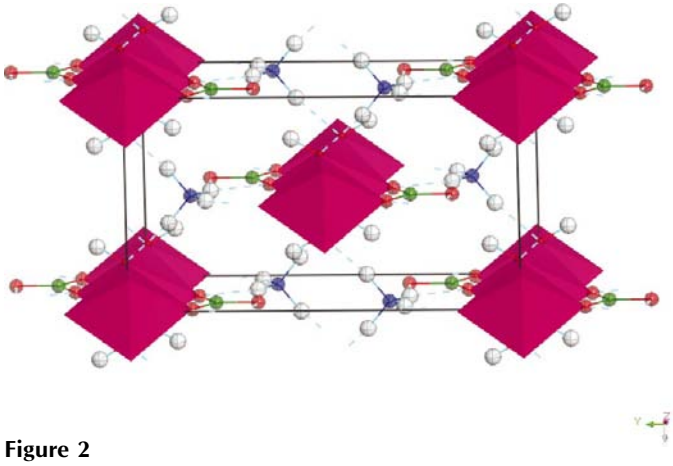

Figure 2
The crystal structure of $(NH_4)Fe(CO_3)(OH)_2$, viewed approximately down the *c* axis.

The Fe—O bonds have both ionic and covalent character. The Fe charge is 1.27, the carbonate O5 charge is −0.62, and the hydroxyl O6 charge is −0.79. The overlap population in the two Fe—O5 carbonate bonds is 0.28 electrons, and that in the four Fe—O6 hydroxyl bonds is 0.24 electrons.

The orientations of the hydroxyl groups and the ammonium cations are determined by hydrogen bonding. The hydroxyl group acts as a hydrogen donor to the carbonate oxygen O4 of an adjacent chain. The ammonium hydrogen H8 forms hydrogen bonds to both carbonate oxygen atoms, and H9 forms a single hydrogen bond to the hydroxyl oxygen O6. Comparing the non-bonded overlap populations to those of the O—H and N—H covalent bonds (Table 3) indicates that the hydrogen bonds contribute significant energy to the structure.

2.6. Conclusions

Synthesis of $(NH_4)Fe(CO_3)(OH)_2$ requires CO_2 and H_2O, neither of which should have been present in the liquid-ammonia feed system. After careful examination of the system for leaks (and finding none), we concluded that these deposits were a startup problem, rather than a failure of the system. While the details of the crystal structure were not critical for answering the technical service question, encountering an incompletely characterized compound presented an irresistible opportunity.

3. $[Al(H_2O)_6][Al(H_2O)_5(SO_4)](H_3O)_2(SO_4)_5$

3.1. Background

A black tar was recovered from a pump seal at an alkylation unit at one of BP's refineries. The process engineers were concerned that sulfuric acid had leaked into this pump, which had an aluminium housing. The powder pattern (Fig. 3) indicated that this tar contained the crystalline phases $Al_4H_2(SO_4)_7(H_2O)_{24}$ (PDF entry 22-6), szomolnokite, $FeSO_4(H_2O)$ (PDF entry 74-1332), and alunogen, $Al_2(SO_4)_3(H_2O)_{17}$ (PDF entry 26-1010). The amorphous hydrocarbon present in the tar could be removed by washing with acetone. The crystal structure of $Al_4H_2(SO_4)_7(H_2O)_{24}$ had not been reported, so before the Rietveld analysis (for quantification) could be carried out, the structure had to be derived.

3.2. Determination of the structure

Among the most useful features of the ICSD is the ability to search on the 'structure type' (designated ANX). In the ANX formula, elements with positive oxidation state are symbolized by the first letters of the alphabet A–M, elements with a negative oxidation state are symbolized by the last letters of the alphabet S–Z, and elements with an oxidation state of 0 are symbolized by the letters N–R. The letters are sorted within the groups according to increasing index (AB2X4, not A2BX4). Structures that contain more than four positive,

Table 3
Hydrogen bonds in $(NH_4)Fe(CO_3)(OH)_2$.

	O—H (Å)	H···O (Å)	O—H···O (°)	O—H overlap (electron)	H···O overlap (electron)
O6—H7···O4	0.989	1.960	161.2	0.58	0.06
N2—H8···O4	1.041	2.171	140.5	0.62	0.02
N2—H8···O5	1.041	2.024	155.8	0.62	0.04
N2—H9···O6	1.045	1.892	168.5	0.67	0.07

three negative, or three neutral types of atoms are not considered. The ANX formula is calculated only for fully determined structures and hydrogen atoms are not considered.

By the conventions of the ICSD, $Al_4H_2(SO_4)_7(H_2O)_{24}$ has the formula type ANX = A4B7X52. At the time of this work, the ICSD contained only one entry with this formula type, $Cr_4H_2(SO_4)_7(H_2O)_{24}$. Although the powder pattern of this chromium compound (PDF entry 72-981) does not appear to match that of the aluminium compound very well (both patterns are available as a supplementary figure), the two compounds are in fact isostructural. Substituting Al for Cr in the reported structure (Gustafsson *et al.*, 1980) led to an excellent Rietveld refinement of the structure of the Al compound. Since this problem was solved, a single-crystal structure of $Al_4H_2(SO_4)_7(H_2O)_{24}$ has been included in the ICSD (Fischer *et al.*, 1996).

3.3. Refinement of the structure

The crystal structure of $Al_4H_2(SO_4)_7(H_2O)_{24}$ was refined. Soft constraints of 1.91 (2) Å were applied to the Al—O bonds, 1.47 (1) Å to the S—O bonds, 2.40 (2) Å to the sulfate O···O non-bonded distances, and 2.70 (3) Å to the O···O non-bonded distances in the AlO_6 coordination spheres. All heavy atoms were refined isotropically; the displacement coefficients were constrained by atom type. The structures of szomolnokite and alunogen were not refined.

Although the hydrogen positions had been determined in szomolnokite (Wildner & Giester, 1991), the H atoms in $Cr_4H_2(SO_4)_7(H_2O)_{24}$ and alunogen (Fang & Robinson, 1976) had not been reported. Since hydrogen accounts for 4.2 wt% of $Al_4H_2(SO_4)_7(H_2O)_{24}$ and 5.2 wt% of alunogen, it was important to include the H atoms in the structure models to obtain the most accurate quantitative analysis. By examination of the O···O distances, the hydrogen-bonding patterns could be deduced. The H atoms were placed on the O···O vectors, 0.97 Å from the covalently bonded oxygen.

Scale factors for all three phases and the lattice parameters of $Al_4H_2(SO_4)_7(H_2O)_{24}$ and szomolnokite were refined. The peak profiles were described by the Thompson–Cox–Hastings pseudo-Voigt profile function number 2. For $Al_4H_2(SO_4)_7(H_2O)_{24}$, the Cauchy X size broadening term was refined, and for szomolnokite, both X and the Cauchy strain broadening coefficient Y were refined. Also refined was a common specimen displacement parameter. The background was described by a three-term cosine Fourier series.

The final refinement of 118 variables using 4069 observations yielded the residuals R_{wp} = 0.0757, R_p = 0.0575, $R(F)$ = 0.0336, $R(F^2)$ = 0.0583, and χ^2 = 2.671. The slope and intercept of the normal probability plot were 1.487 and 0.0423, respectively. The soft constraints contributed 5% to the final reduced χ^2. The agreement of the observed and calculated patterns (Fig. 4) is excellent.

Attempts to optimize the hydrogen positions using force-field techniques (with the heavy atoms fixed) did not yield chemically reasonable results. Quantum-chemical optimizations of the $Al_4H_2(SO_4)_7(H_2O)_{24}$ and alunogen structures were carried out using *CASTEP* (Millman *et al.*, 2000). The lattice parameters were fixed, but the positions of all atoms were allowed to refine. The geometry optimization was carried out at the CGA-PW91 level of theory, with an 0.05 $Å^{-1}$ k-point spacing (one- or two-point sampling of the Brillouin zone of the primitive unit cell). The compounds were treated as metals and the number of default orbitals was increased by 10% to include some empty orbitals in the calculation. To cope with the disordered sulfate in $Al_4H_2(SO_4)_7(H_2O)_{24}$, the structure was optimized twice in space group $P1$, with the two different orientations of the sulfate. The energies of the structures with the two orientations differed by only 0.7 kJ $mol.^{-1}$. There is every reason to believe that the sulfate is really disordered, and not that the disorder is an artifact of the crystallography.

Both the refined and optimized atom coordinates for $Al_4H_2(SO_4)_7(H_2O)_{24}$ are available in CIF format. The reported optimized coordinates are the averages of the symmetry-related positions in space group $P\bar{1}$. The optimized atom coordinates for alunogen are also available in CIF format.

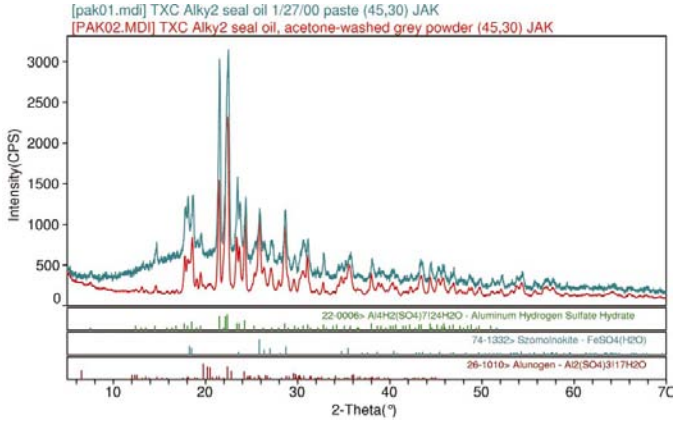

Figure 3
Powder patterns of an as-received pump seal deposit, and after removing the organic components with acetone.

3.4. Description of the $Al_4H_2(SO_4)_7(H_2O)_{24}$ structure

The structure of $Al_4H_2(SO_4)_7(H_2O)_{24}$ (Fig. 5) contains two independent aluminium atoms: one is an $Al(H_2O)_6^{3+}$ cation, while the other is coordinated to five water molecules and one monodentate sulfate anion. One of the 'waters of solvation' in the asymmetric unit is actually a hydronium ion. One of the four independent sulfate anions is disordered. The correct formulation of this compound is thus $[Al(H_2O)_6]_2[Al(H_2O)_5(SO_4)]_2(H_3O)_2(SO_4)_5$. The Al1—O19(S5) bond [1.880 (12) Å] is not significantly longer than the Al—OH_2 bonds [average 1.880 (35) Å]. Likewise, the S5—O19(Al1) bond of 1.464 (8) Å does not differ significantly from the average of the other ordered S—O bonds [1.468 (7) Å].

3.5. Hydrogen bonding in $Al_4H_2(SO_4)_7(H_2O)_{24}$ and alunogen

For analysis of the hydrogen bonding, the optimized structures were used. The structure is dominated by strong hydrogen bonds (Table 4); each H_2O molecule and the H_3O^+ donate protons to sulfate or water O atoms. Among the ordered sulfates, each oxygen (except the coordinated oxygen O19) accepts two protons. The average O—H bond length is 1.001 (16) Å, the average H···O distance is 1.685 (120) Å, and the average O—H···O angle is 171 (7)°. These values are typical for strong O—H···O hydrogen bonds (Jeffrey, 1997). The average overlap population in the covalent O—H bonds is 0.51 (2) electrons, and the average overlap population in the hydrogen bonds is 0.11 (3) electrons. The hydrogen bonds formed by the hydronium ion O31/H51/H52/H53 are stronger [O—H = 1.029 (17), H···O = 1.525 (86) Å, 0.46 (1) and 0.17 (2) electrons] than those of the water molecules. Each orientation of the disordered sulfate S6/O7/O8/O9/O10 is involved in only three hydrogen bonds, and these are more bent [O—H···O = 148 (8)°] than those to the other sulfates. This weaker bonding to the rest of the structure explains the disorder of this sulfate anion.

The hydrogen bonds in the alunogen structure (Table 5) are similar to those in $Al_4H_2(SO_4)_7(H_2O)_{24}$. Each hydrogen in the coordinated (O18–O29) and the solvated (O30–O34) water molecules participates in a hydrogen bond. Most of the sulfate O atoms accept two protons. O17 participates in three weaker hydrogen bonds, and at O11 one of the three hydrogen bonds is much weaker than the other two. The water molecule O31 participates in two water–sulfate hydrogen bonds, while the other waters of solvation form a water–water and a water–sulfate hydrogen bond. The average O—H bond distance is 0.999 (12) Å, the H···O distance is 1.68 (11) Å, and the O—H···O angle is 170 (9)°. The average overlap population in the O—H covalent bonds is 0.51 (1) electrons, and the overlap population in the H···O bonds is 0.10 (3) electrons. The result of this hydrogen bonding is the formation of double layers of $Al(H_2O)_6$/sulfate and sulfate/water layers, which alternate along the *b* axis.

3.6. Conclusions

From the refined scale factors, the crystalline portion of this deposit contained 70% $Al_4H_2(SO_4)_7(H_2O)_{24}$, 22% $FeSO_4(H_2O)$, and 8% $Al_2(SO_4)_3(H_2O)_{17}$. The Fe/S ratio calculated from these concentrations agreed well with the value of 0.27 determined by bulk chemical analysis. The Al/Fe and Al/S ratios of 2.02 and 0.45 were lower than the bulk values (2.76 and 0.75, respectively). We concluded that the amorphous portion of the deposit contained aluminium. By combining the bulk chemical analysis with the Rietveld results, the true concentrations of these three phases in the whole deposit were 23, 7 and 3 wt%, respectively.

The most complete investigation of the $Al_2(SO_4)_3$–H_2SO_4–H_2O system (Taylor & Bassett, 1952) indicates that this phase is formed around 323–333 K at $H_2SO_4/Al_2(SO_4)_3$ ratios from 2.4 to 14.5: acid-rich conditions. It was obtained by slow transformation of $Al_2(SO_4)_3(H_2O)_{16}$ or $Al_2H_2(SO_4)_4(H_2O)_{12}$,

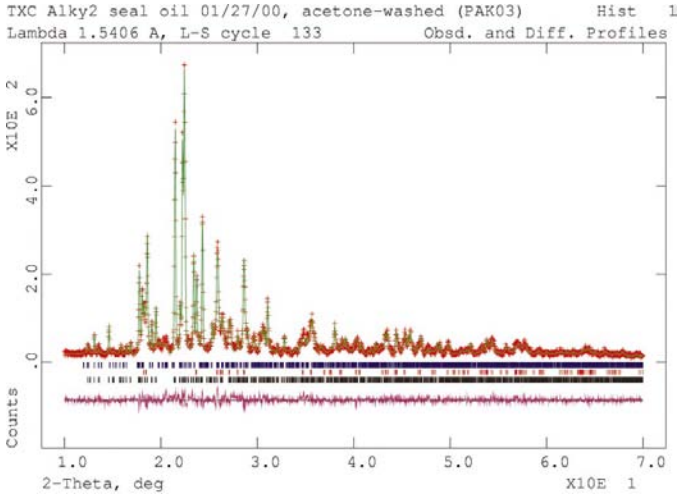

Figure 4
Observed, calculated and difference patterns of the pump seal deposit. The small crosses represent the observed data points and the smooth line through them the calculated pattern. The difference pattern is plotted at the same scale as the other patterns.

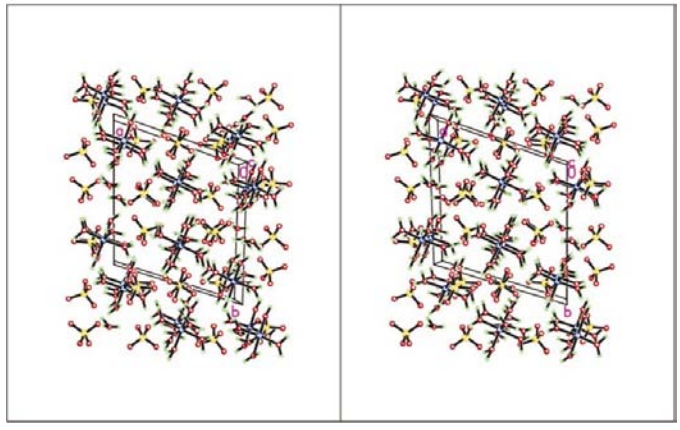

Figure 5
The crystal structure of $Al_4H_2(SO_4)_7(H_2O)_{24}$, viewed down the *a* axis. The disordered sulfate is located at $\frac{1}{2}$, 0, 0.

Table 4
Hydrogen bonds in $Al_4H_2(SO_4)_7(H_2O)_{24}$.

	O—H (Å)	H···O (Å)	O—H···O (°)	O—H overlap (electron)	H···O overlap (electron)
O23—H35···O7	0.995	1.741	134.2	0.51	0.13 (1)
O23—H35···O8	0.995	2.248	123.8	0.51	−0.01 (2)
O23—H35···O9	0.995	1.729	154.7	0.51	0.14 (2)
O23—H35···O10	0.995	2.150	122.9	0.51	−0.01 (1)
O23—H36···O13	0.994	1.649	177.9	0.52	0.11
O24—H37···O15	0.988	1.842	171.6	0.54	0.08
O24—H38···O21	1.007	1.596	176.3	0.52	0.13
O25—H39···O12	1.001	1.680	165.9	0.51	0.12
O25—H40···O22	0.982	1.965	143.7	0.54	0.06
O26—H41···O8	0.989	1.570	156.2	0.51	0.18 (2)
O26—H41···O9	0.989	1.958	146.9	0.51	0.09 (1)
O26—H42···O15	0.994	1.722	175.2	0.51	0.11
O27—H43···O11	1.003	1.621	168.0	0.51	0.13
O27—H44···O16	1.001	1.637	169.1	0.52	0.11
O28—H45···O15	0.988	1.885	173.1	0.52	0.08
O28—H46···O21	0.997	1.707	173.3	0.53	0.09
O29—H47···O11	0.970	1.743	168.5	0.52	0.10
O29—H48···O18	1.004	1.626	172.7	0.52	0.12
O30—H49···O18	1.007	1.578	176.2	0.51	0.14
O30—H50···O22	1.001	1.630	168.2	0.52	0.12
O31—H51···O12	1.040	1.455	174.2	0.45	0.18
O31—H52···O14	1.010	1.622	167.8	0.47	0.14
O31—H53···O17	1.038	1.500	174.7	0.45	0.18
O32—H54···O13	1.000	1.679	176.0	0.51	0.10
O32—H55···O16	1.010	1.777	172.8	0.52	0.08
O33—H56···O14	0.992	1.803	175.1	0.52	0.09
O33—H57···O20	1.005	1.629	174.1	0.51	0.12
O34—H58···O7	0.987	1.808	145.6	0.47	0.20 (1)
O34—H58···O10	0.987	1.564	149.5	0.47	0.13 (2)
O35—H59···O20	0.991	1.736	167.3	0.53	0.09

and is metastable with respect to $Al_2(SO_4)_3(H_2O)_{14}$. Apparently, sulfuric acid had leaked into the pump and reacted with both the aluminium housing and steel pump parts. The fact that the major phase is metastable with respect to other hydrated aluminium sulfates suggested that the corrosion was current and not an historical event.

This problem was solved in early 2000. At that time the $Cr_4H_2(SO_4)_7(H_2O)_{24}$ structure (Fischer *et al.*, 1996) was not included in the released version of the ICSD; the entry states that it was recorded on 31 December 1999. There is often a significant delay between publication of a structure and its incorporation into a database. To obtain the most complete searches for structures, the current primary literature must also be consulted.

4. Lower hydrates of magnesium chloride

4.1. Background

The normally encountered hydrate of magnesium chloride is $MgCl_2(H_2O)_6$, found in nature as the mineral bischofite (PDF entry 22-515). A dodecahydrate has also been characterized structurally (Sasvari & Jeffrey, 1966), and an octahydrate has been reported (van't Hoff & Meyerhoffer, 1898). Three lower hydrates, $MgCl_2(H_2O)$ (PDF 1-947, CAS 22756-14-5; Hanawalt *et al.*, 1938), $MgCl_2(H_2O)_2$ (PDF 3-765, CAS 19098-17-0; Dow Chemical Company), and $MgCl_2(H_2O)_4$ (PDF 1-1210, CAS 22695-80-3; Dow Chemical Company), have been reported. Although some chemical and physical properties of these three compounds have been reported, the only reference to these compounds in the crystallographic literature is in the PDF.

The hexahydrate crystallizes from aqueous solution between 270 and 390 K (de Marignac, 1856; Mellor, 1923). The tetrahydate has been prepared by passing HCl into a solution of magnesium chloride (Lescoeur, 1894), or by dehydrating the hexahydrate at elevated temperatures. The dihydrate has been made only in the presence of excess HCl (Ditte, 1881; van't Hoff & Meyerhoffer, 1898). The monohydrate was prepared by passing HCl over the hexahydrate at 408 K (Moldenhauer, 1906).

From time to time, in our studies of polypropylene catalysts and catalyst precursors, we encounter materials having powder patterns which match those of these three lower hydrates of magnesium chloride. To apply the Rietveld method, structural models are necessary. Suitable models for all three phases could be located in the ICSD and the structures refined.

4.2. Experimental

Two samples, isolated from preparations of polypropylene catalysts, were front-loaded into sample holders in a glove box. The moisture-sensitive samples were protected from the atmosphere by attaching a 3 μm thick polycarbonate film to the holders with silicone grease. Patterns were measured (Cu $K\alpha$ radiation, 3–60/80° 2θ, 0.04° steps, 24/32 s step^{-1}) on a Scintag PAD V diffractometer equipped with an Ortec intrinsic Ge detector. One sample was identified as moderately crystalline tetrahydrate, and the other as containing a mixture of poorly crystalline dihydrate and monohydrate [the observed powder patterns of $MgCl_2(H_2O)_4$, which contained a Si internal standard, and of a mixture of $MgCl_2(H_2O)_2$ and $MgCl_2(H_2O)$ have been deposited].

4.3. Determination of the structures

4.3.1. $MgCl_2(H_2O)_4$. A Mg^{2+} cation is similar in size and charge to several divalent first-row transition metal cations, and Mg compounds are often isostructural to those of transition metals. The ICSD formula type ANX of the tetrahydrate is AX2Y4. A search for compounds having this formula type and containing hydrogen, oxygen and a halogen yielded several divalent metal halide tetrahydrates in space

Table 5
Hydrogen bonds in alunogen, $Al_2(SO_4)(H_2O)_{17}$.

	O—H (Å)	H···O (Å)	O—H···O (°)	O—H overlap (electron)	H···O overlap (electron)
O18—H35···O16	0.994	1.675	175.9	0.52	0.11
O18—H36···O32	1.015	1.563	171.5	0.49	0.16
O19—H37···O6	1.005	1.615	173.8	0.52	0.12
O19—H38···O16	1.003	1.605	163.4	0.51	0.13
O20—H39···O9	1.003	1.643	176.6	0.51	0.12
O20—H40···O7	0.999	1.674	172.4	0.52	0.11
O21—H41···O7	1.000	1.678	179.0	0.52	0.11
O21—H42···O8	1.005	1.631	173.2	0.52	0.12
O22—H43···O6	0.998	1.605	174.9	0.52	0.13
O22—H44···O31	1.015	1.606	175.9	0.50	0.14
O23—H45···O8	1.002	1.636	176.5	0.51	0.12
O23—H46···O9	0.999	1.681	172.8	0.52	0.11
O24—H47···O15	0.998	1.695	175.7	0.52	0.11
O24—H48···O33	1.020	1.555	175.2	0.51	0.11
O25—H49···O11	0.995	1.715	173.9	0.53	0.10
O25—H50···O14	1.010	1.610	178.2	0.50	0.14
O26—H51···O12	1.004	1.649	172.7	0.51	0.12
O26—H52···O13	1.002	1.654	173.8	0.51	0.12
O27—H53···O10	0.999	1.677	176.4	0.52	0.11
O27—H54···O12	1.005	1.617	172.5	0.52	0.12
O28—H55···O11	0.995	1.684	174.8	0.53	0.11
O28—H56···O30	1.028	1.495	175.9	0.48	0.18
O29—H57···O10	0.997	1.672	172.7	0.52	0.11
O29—H58···O13	1.001	1.640	173.8	0.51	0.12
O30—H59···O17	0.983	1.898	178.8	0.52	0.06
O30—H60···O33	0.984	1.956	157.2	0.51	0.06
O31—H61···O15	0.996	1.736	170.7	0.50	0.10
O31—H62···O17	0.994	1.723	163.9	0.52	0.09
O32—H63···O14	0.983	1.983	158.8	0.51	0.05
O32—H64···O31	0.986	1.897	166.7	0.51	0.08
O33—H65···O11	0.976	2.418	149.6	0.51	0.02
O33—H66···O34	1.012	1.613	171.8	0.48	0.14
O34—H67···O17	0.979	1.911	148.6	0.52	0.05
O34—H68···O32	0.976	2.325	141.3	0.52	0.02

group $P2_1/c$, including a neutron single-crystal study of $FeCl_2(H_2O)_4$ (Verbist *et al.*, 1972). This structure proved to be a suitable initial model.

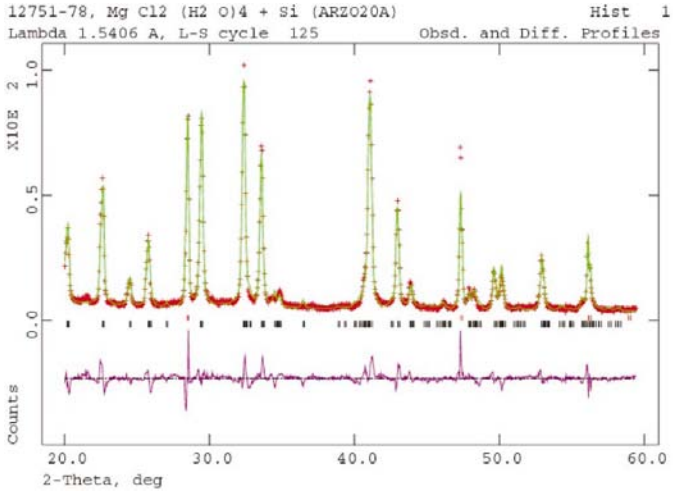

Figure 6
Observed, calculated and difference patterns of $MgCl_2(H_2O)_4$. The small crosses represent the observed data points, and the smooth line through them the calculated pattern. The difference pattern is plotted at the same scale as the other patterns.

4.3.2. $MgCl_2(H_2O)_2$. A search for compounds with the formula type AX2Y2, containing H_4O_2 and containing only four elements, yielded several divalent metal dihalide dihydrates which crystallize in space group $C2/m$, including a neutron single-crystal study of $CoCl_2(H_2O)_2$ (Cox *et al.*, 1965). This proved to be a suitable initial model.

4.3.3. $MgCl_2(H_2O)$. This stoichiometry is relatively uncommon. A search for compounds having formula type AXY2, containing H_2O, and only four elements yielded 18 hits, all in space group *Pnma*. Most of these are salts of large alkaline earth cations, but among the hits was $CdCl_2(H_2O)$ (Leligny & Monier, 1974), which proved to be a suitable initial model.

4.4. Refinement of the structures

4.4.1. $MgCl_2(H_2O)_4$. All data processing was carried out using *GSAS* (Larson & Von Dreele, 1998). To minimize the effects of incomplete interception of the beam at low angles, surface roughness, and the effect of the polycarbonate window, only the 20–60° portion of the pattern was included in the refinement. A single isotropic displacement coefficient was refined for the non-H atoms. Soft constraints of 2.52 (2) and 2.08 (3) Å were applied to the Mg—Cl and Mg—O bonds, respectively. Scale factors for magnesium chloride tetrahydrate and the silicon internal standard were refined, as well as the lattice parameters of the chloride. Preferred orientation was described by second-order spherical harmonics. The profiles were described by profile function number 2; a Cauchy size broadening term X was refined for each phase, as well as common *trns*, *asym* and *shift*. The background was described by an eight-term real-space pair-correlation function, with fixed distances of 2.6, 6.6 and 9.0 Å.

The final refinement of 29 variables using 992 observations yielded the residuals $R_{wp} = 0.1302$, $R_p = 0.0988$, $R(F) = 0.0900$, $R(F^2) = 0.3247$, and $\chi^2 = 6.366$. The slope and intercept of the normal probability plot were 2.203 and 0.157, respectively. The soft constraints contributed 0.5% to the final reduced χ^2. The agreement of the observed and calculated patterns (Fig. 6) is relatively poor. The largest errors probably result from incomplete powder averaging and the poor quality of the only available data.

A quantum-chemical optimization of the structure was carried out using *CASTEP* (Millman *et al.*, 2000). The lattice parameters were fixed, but the positions of all atoms were allowed to refine. The geometry optimization was carried out

at the CGA-PW91 level of theory, with an 0.05 Å^{-1} *k*-point spacing (two-point sampling of the Brillouin zone of the primitive unit cell). The compound was treated as a metal and the number of default orbitals was increased by 10% to include some empty orbitals in the calculation. The refined and optimized coordinates are available in CIF format.

4.4.2. $MgCl_2(H_2O)_2$ and $MgCl_2(H_2O)$. All data processing was carried out using *GSAS* (Larson & Von Dreele, 1998). To minimize the effects of incomplete interception of the beam at low angles, surface roughness and the effect of the window, only the 20–80° portion of the pattern was included in the refinement. Fixed isotropic displacement coefficients were used for all atoms. Soft constraints of 2.55 (2) and 2.02 (3) Å were applied to the Mg—Cl and Mg—O bonds, respectively. Scale factors and lattice parameters were refined for both phases. The profiles were described by profile function number 2; a Cauchy size broadening term *X* was refined for each phase, as well as a common specimen displacement coefficient. The background was described by a four-term real-space pair-correlation function, with a fixed distance of 1.27 Å.

The final refinement of 25 variables using 1910 observations yielded the residuals R_{wp} = 0.0378, R_p = 0.0293, $R(F)$ = 0.0088, $R(F^2)$ = 0.0153, and χ^2 = 1.460. The slope and intercept of the normal probability plot were 1.181 and 0.029, respectively. The soft constraints contributed 0.4% to the final reduced χ^2. The

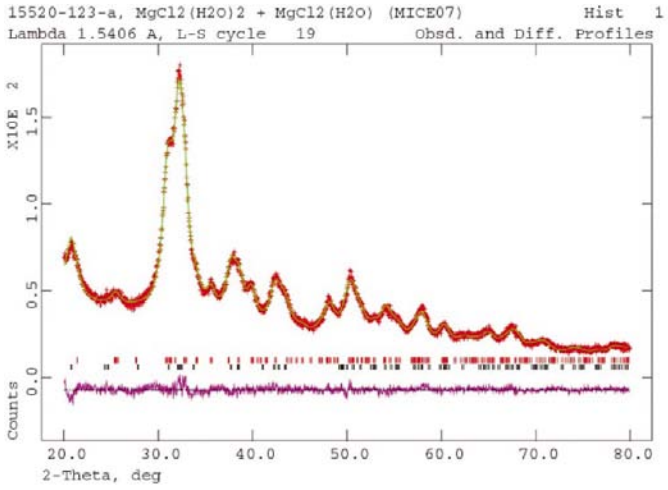

Figure 7
Observed, calculated and difference patterns of the mixture of $MgCl_2(H_2O)_2$ and $MgCl_2(H_2O)$. The small crosses represent the observed data points and the smooth line through them the calculated pattern. The difference pattern is plotted on the same scale as the other patterns.

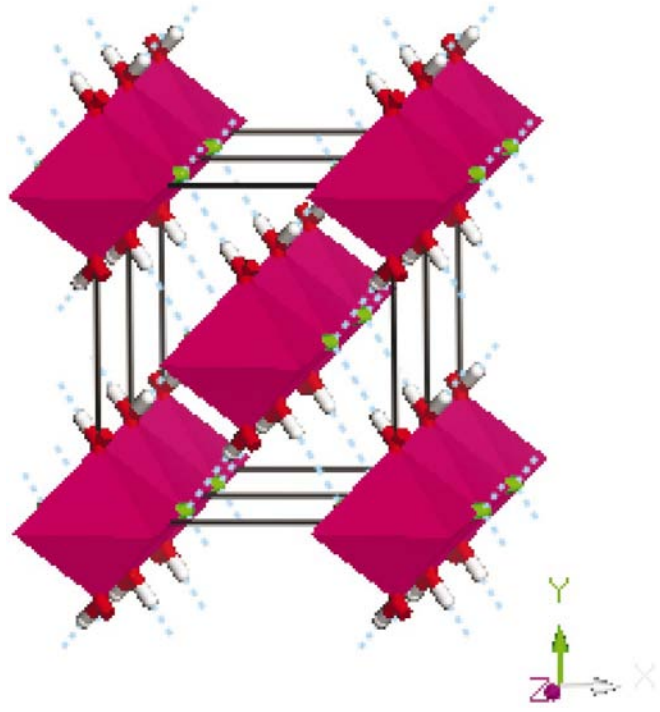

Figure 9
The crystal structure of $MgCl_2(H_2O)_2$, viewed approximately down the *c* axis.

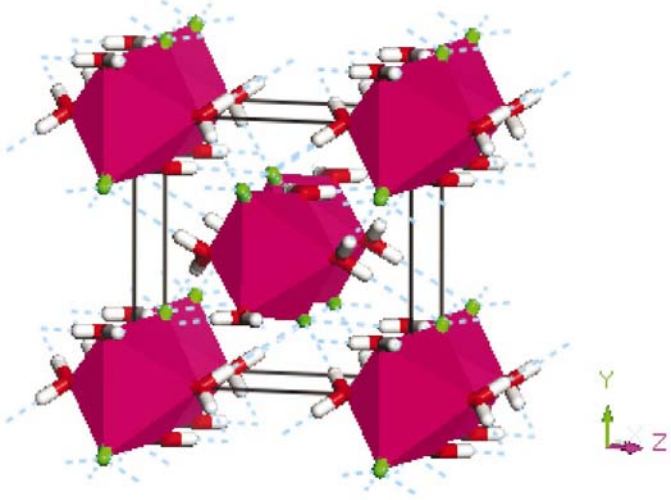

Figure 8
The crystal structure of $MgCl_2(H_2O)_4$, viewed approximately down the *a* axis.

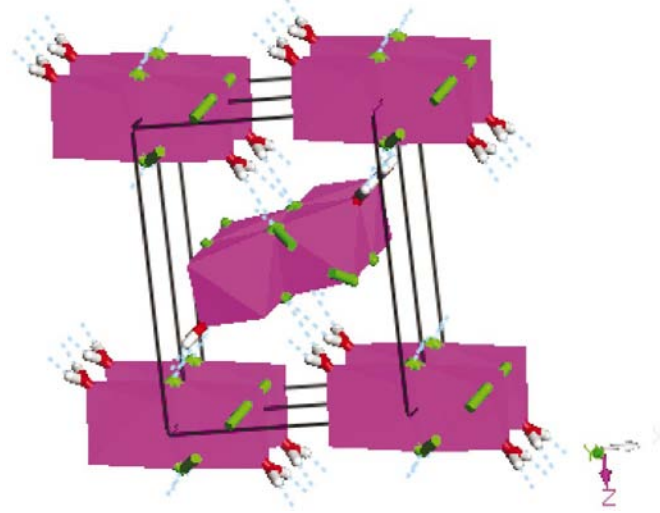

Figure 10
The crystal structure of $MgCl_2(H_2O)$, viewed approximately down the *b* axis.

Table 6
Bonding in $MgCl_2(H_2O)_n$.

	$n = 6$	$n = 4$	$n = 2$	$n = 1$	$n = 0$
No. of coordinated Cl	0	2	4	5	6
Mg charge	1.85	1.67	1.49	1.38	1.24
Cl charge	−0.65	−0.65	−0.66	−0.70 −0.63	−0.62
O charge	−1.04, −1.04	−1.04, −1.03	−1.03	−1.01	–
H charge	0.47, 0.49, 0.46, 0.48	0.47, 0.47, 0.46, 0.47	0.47	0.48	–
Mg—Cl (Å)	–	2.572, −0.23	2.546, −0.49	2.390, −0.97 2.620, −0.33	2.503, −0.88
Mg—O (Å)	2.125, −0.80 2.076, −1.01	2.090, −0.92 2.103, −0.92	2.049, −1.10	2.057, −1.11	–
O—H (Å)	0.985, 0.52 0.976, 0.53 0.988, 0.52 0.978, 0.53	0.985, 0.52 0.986, 0.52 0.986, 0.53 0.985, 0.52	0.984, 0.53	0.976, 0.54	–
O—H···Cl (°)	2.177 174.0 0.08 2.460 142.7 0.04 2.154 173.5 0.09 2.488 141.4 0.04	2.246 172.8 0.07 2.215 172.8 0.07 2.162 166.4 0.07 2.183 164.3 0.07	2.195 167.6 0.07	2.410 152.6 0.04	– – –

Table 7
Energetics of $MgCl_2(H_2O)_n$.

n	ΔH_f (kJ mol^{-1})	$\Delta\Delta H_f$ (kJ mol^{-1})		E (eV)	ΔE (eV)	
0	−641.8	0		−1803.8690637	0	
1	−968.6	−326.8		−2275.0340503	−471.1649806	
2	−1280.3	−311.7		−2746.8616462	−471.8275959	
4	−1899.5	−619.2	−309.6	−3689.8458686	−942.9842224	−471.4921112
6	−2499.6	−600.1	−300.0	−4632.4701193	−942.6242507	−471.3121254
Average $\Delta E/H_2O$		−312.0 (111)			−471.4492033 (2855521)	

agreement of the observed and calculated patterns (Fig. 7) is excellent.

Quantum-chemical optimizations of both structures were carried out using *CASTEP* (Millman *et al.*, 2000). The lattice parameters were fixed, but the positions of all atoms were allowed to refine. The geometry optimization was carried out at the CGA-PW91 level of theory, with a 0.05 Å^{-1} k-point spacing (six/two-point sampling of the Brillouin zone of the primitive unit cell). The compounds were treated as metals and the number of default orbitals was increased by 10% to include some empty orbitals in the calculation. The refined and optimized coordinates are available in CIF format. Calculated powder patterns of all three compounds have been submitted to the ICDD for inclusion in future releases of the Powder Diffraction File.

4.5. Descriptions of the structures

The structure of $MgCl_2(H_2O)_4$ (Fig. 8) consists of discrete mononuclear complexes of octahedral Mg^{2+} cations. The Cl ligands occupy the axial positions, and the water molecules the equatorial positions of the coordination sphere. The Mg—Cl bond distance is 2.522 (8) Å, and the Mg—O distances are 2.04 (2) and 2.11 (2) Å; all are within normal ranges. The angular deviations from the ideal octahedral geometry are < 3°.

In magnesium chloride dihydrate (Fig. 9) there are edge-sharing chains of octahedral Mg parallel to the *c* axis. The doubly bridging Cl occupy the equatorial positions and the water molecules occupy the axial positions of the coordination sphere. The Mg—Cl distances are 2.570 (5) and 2.530 (8) Å, and the Mg—O distance is 2.02 (2) Å. The deviations from the ideal octahedral geometry are < 2°.

The structure of $MgCl_2(H_2O)$ (Fig. 10) consists of double chains (parallel to the *b* axis) of edge-sharing Mg octahedra. Between the Mg are triply bridging Cl3, and on the outer portions of the chains are doubly bridging Cl2. A single water molecule is coordinated to each cation. The Mg—Cl distances to the triply bridging Cl are 2.537 (12) and 2.468 (16) Å; the distance to the doubly bridging Cl is 2.461 (12) Å. The Mg—O distance is 2.01 (2) Å.

The bonding in these three compounds, and in $MgCl_2(H_2O)_6$ (Agron & Busing, 1969) and $MgCl_2$ (Partin & O'Keefe, 1991), is almost completely ionic (Table 6). The overlap populations in the Mg—Cl and Mg—O bonds are negative. The charge in the Mg decreases as the number of coordinated Cl atoms increases. The $MgOH_2$ units in all three compounds are nearly planar; the sums of the angles around the oxygen are 359.8/345.6, 360.1 and 359.2° for the tetrahydrate, dihydrate and monohydrate, respectively.

Hydrogen bonding is important in all three structures. All hydrogen bonds that *can* form, *do* form. In the tetrahydrate each water molecule donates each proton to the coordinated chloride, which thus participates in four hydrogen bonds. The Cl in the dihydrate participates in two hydrogen bonds. In the monohydrate the hydrogen bonds (2/Cl) are to the triply bridging Cl. The overlap populations of these hydrogen bonds (Table 6) indicate that they are strong.

The calculated absolute energies of these compounds exhibit an excellent correlation to the heats of formation

(Weast, 1978; Table 7). These energy differences provide a way of quantifying the strengths of the hydrogen bonds in this series of compounds. The average energy difference per water molecule is 312 (11) kJ mol^{-1}. When each water molecule is added to the formula, one Mg—Cl bond is broken [327.6 (21) kJ mol^{-1}], and one Mg—O bond [363.2 (126) kJ mol^{-1}; Lide, 1999] and two O—H$\cdots$Cl bonds are formed. The average strength of the hydrogen bond is thus 134.9 kJ mol^{-1}. The average strengths of O—H and H—Cl covalent bonds are 427.6 and 431.6 kJ mol^{-1}, respectively. The average O—H bond overlap population is 0.53 (1) electrons, and the average overlap population of the hydrogen bonds is 0.06 (2) electrons. The 'bond energy' is approximately proportional to the square root of the overlap population. This relationship may be a useful 'rule of thumb' for estimating the strengths of hydrogen bonds.

4.6. Conclusions

As the H_2O/Mg ratio decreases, the structures resemble progressively larger pieces of the $MgCl_2$ structure. With a good initial structural model, accurate (if not very precise) structural information can be obtained, even from poor data. Computational techniques are becoming more useful for completing structures and understanding the solid-state bonding.

5. General conclusions

Most diffractionists use the PDF as their primary database tool for phase identification. Even though powder patterns calculated from ICSD entries are now included in the PDF, neither it nor any other database can solve every problem encountered by the analyst. As these examples demonstrate, the information in the ICSD is very useful for 'solving' crystal structures by analogy. This author uses the ICSD daily to answer business-related questions.

Often, complaints are heard about the costs of the crystallographic databases. The complainers need to understand that collection and critical evaluation of information are not 'free'; real people and real resources are required. Solution of each of these problems paid for the costs of the databases in saved time and in business impact. The databases are tools every bit as vital as the personal computer. A real challenge for all of the database organizations, though, is to make possible on-line access for the occasional user, without jeopardizing their financial stability.

References

Agron, P. A. & Busing, W. R. (1969). *Acta Cryst.* A**25**, S118–S119.
Allen, F. H. (2002). *Acta Cryst.* B**58**, 380–388.
Belsky, A., Hellenbrandt, M., Karen, V. L. & Luksch, P. (2002). *Acta Cryst.* B**58**, 364–369.
Bergerhoff, G., Hundt, R., Sievers, R, & Brown, I. D. (1983). *J. Chem. Inf. Comput. Sci.* **23**, 66–69.
Berman, H. M., Battistuz, T., Bhat, T. N., Bluhm, W. F., Bourne, P. E., Burkhardt, K., Zukang, F., Gilliland, G. L., Iype, L., Jain, S., Fagan, P., Marvin., J., Ravichanran, V., Schneider, B., Thanki, N., Padilla, D., Weissig, H., Westbrook, J. D. & Zardecki, C. (2002). *Acta Cryst.* B**58**, 899–907.
Bruno, I. J., Cole, J. C., Edgington, P. R., Kessler, M., Macrae, C. F., McCabe, P., Pearson, J. & Taylor, R. (2002). *Acta Cryst.* B**58**, 389–397.
Cox, D. E., Frazer, B. C. & Shirane, G. (1965). *Phys. Lett.* **17**, 103–104; ICSD collection code 60263.
Ditte, A. (1881). *Ann. Chim. Phys.* **22**, 560–565.
Dvořák, V. & Feitknecht, W. (1969). *Helv. Chim. Acta*, **52**, 515–522.
Erdös, E. & Altorfer, H. (1976). *Werkst. Korros.* **27**, 611–618.
Faber, J. & Fawcett, T. (2002). *Acta Cryst.* B**58**, 325–332.
Fang, J. H. & Robinson, P. D. (1976). *Am. Mineral.* **61**, 311–317; ICSD collection code 12129.
Fischer, T., Kneip, R. & Wunderlich, H. (1996). *Z. Kristallogr.* **211**, 469–470.
Gustafsson, T., Lundgren, J. O. & Olovsson, I. (1980). *Acta Cryst.* B**36**, 1323–1326; ICSD collection code 16449.
Hanawalt, J., Rinn, H. & Frevel, L. (1938). *Anal. Chem.* **10**, 457–512.
Hoff, J. H. van't & Meyerhoffer, W. (1898). *Z. Phys. Chem.* **13**, 459–466.
Iga, T. & Kato, S. (1978). *J. Ceram. Soc. Jpn*, **86**, 509–512; ICSD collection code 36397.
Jeffrey, G. A. (1997). *An Introduction to Hydrogen Bonding.* Oxford University Press.
Larson, A. C. & Von Dreele, R. B. (1998). *GSAS*. Los Alamos National Laboratory, Los Alamos, NM, USA.
Leligny, H. & Monier, J. C. (1974). *Acta Cryst.* B**30**, 305–309; ICSD collection code 2028.
Lescoeur, H. (1894). *Ann. Chim. Phys.* **2**, 78.
Lide, D. R. (1999). *CRC Handbook of Chemistry and Physics*, 80th ed., pp. 9–51/56. Boca Raton, FL: CRC Press.
Marignac, J. C. G. de (1856). *Ann. Mines.* **9**, 3–7.
Mellor, J. W. (1923). *A Comprehensive Treatise on Inorganic and Theoretical Chemistry*. London: Longmans Green.
Millman, V., Winkler, B., White, J. A., Pickard, C. J., Payne, M. C., Akhmatskaya, E. V. & Nobes, R. H. (2000). *Int. J. Quantum Chem.* **77**, 895–910.
Moldenhauer, W. (1906). *Z. Anorg. Chem.* **51**, 369–373.
National Institute of Standards and Technology (1997). Standard Reference Data Program, 100 Bureau Dr. Stop 2310, Gaithersburg, MD 20899–2310, USA.
Partin, D. E. & O'Keefe, M. (1991). *J. Solid State Chem.* **95**, 176–183; ICSD collection code 86439.
Powder Diffraction File (2001). International Centre for Diffraction Data, 12 Campus Blvd, Newtown Square, PA 19073-3273, USA.
Sasvari, K. & Jeffrey, G. (1966). *Acta Cryst.* **20**, 875–881.
Taylor, D. & Bassett, H. (1952). *J. Chem. Soc.* pp. 4431–4442.
Verbist, J. J., Hamilton, W. C., Koetzle, T. F. & Lehman, M. S. (1972). *J. Chem. Phys.* **56**, 3257–3264; ICSD collection code 9488.
Visser, J. W. (1969). *J. Appl. Cryst.* **2**, 89–95.
Weast, R. C. (1978). *CRC Handbook of Chemistry and Physics*, 59th ed., pp. D-72. West Palm Beach, FL: CRC Press.
White, P. S., Rodgers, J. R. & Le Page, Y. (2002). *Acta Cryst.* B**58**, 343–348.
Wildner, M. & Giester, G. (1991). *Neues Jahrb. Mineral. Monatsh.* pp. 296–306; ICSD collection code 71345.